

# Leonardo, a Drosophila 14-3-3 Protein Involved in Learning, Regulates Presynaptic Function

Kendal Broadie,\* Emma Rushton,\*  
Efthimios M. C. Skoulakis,<sup>†</sup> and Ronald L. Davis<sup>†</sup>

\*Department of Biology  
University of Utah

Salt Lake City, Utah 84112

<sup>†</sup>Department of Cell Biology and Neurology

Baylor College of Medicine

Houston, Texas 77030

## Summary

The *leonardo* gene encodes a conserved member of the 14-3-3 protein family, which plays a role in *Drosophila* learning. Immunological localization of the protein shows that it is expressed at synaptic connections and enriched in presynaptic boutons of the neuromuscular junction (NMJ). Null *leonardo* mutants die as mature embryos. Electrophysiological assays of the mutant NMJ demonstrate that basal synaptic transmission is reduced by 30% and that transmission amplitude, fidelity, and fatigue resistance properties are reduced at elevated stimulation frequencies and in low external  $[Ca^{2+}]$ . Moreover, transmission augmentation and post-tetanic potentiation (PTP) are disrupted in the mutant. These results suggest that Leonardo plays a role in the regulation of synaptic vesicle dynamics, a function which may underlie synaptic modulation properties enabling learning.

## Introduction

One fruitful approach to identifying proteins participating in synaptic function and plasticity has been the characterization of *Drosophila* mutants defective in olfactory learning and memory (Davis, 1996). The best characterized class of learning mutants are involved in cAMP-dependent signaling, including *dunce*, which encodes a cAMP-dependent phosphodiesterase (Byers et al., 1981); *rutabaga*, which encodes adenylyl cyclase (Levin et al., 1992); *DCO*, which encodes a catalytic subunit of cAMP-dependent protein kinase (Drain et al., 1991); and *dCREB*, which encodes a cAMP-dependent transcription factor (Yin et al., 1994). Many of these same proteins were subsequently implicated in synaptic function and plasticity at the *Drosophila* neuromuscular junction (NMJ; Zhong and Wu, 1991; Zhong et al., 1992; Davis, 1996). This combination of behavioral studies of learning and functional studies of the NMJ has given strong support to the idea that the cAMP cascade plays a central role in learning through participation in synaptic plasticity mechanisms (Davis, 1996). However, it is known that many diverse regulative mechanisms control the expression of synaptic plasticity. Indeed, several additional classes of *Drosophila* learning mutants have been identified, which may encode proteins with important synaptic roles (Davis, 1996). Characterization of mutants through functional and anatomical assays at the NMJ

will be an essential step in elucidating the role of these molecules in the physiology of the synapse.

Recently, we identified a novel *Drosophila* learning mutant, *leonardo*, in a gene that encodes a conserved member of the 14-3-3 protein family (Skoulakis and Davis, 1996). Viable *leonardo* mutants show decreased learning performance correlated to the level of expressed protein; the strongest mutants show a 30% decrement in associative learning (Skoulakis and Davis, 1996). Null *leonardo* mutants die as mature embryos, indicating that the protein also plays an essential function. The *leonardo* protein is highly expressed in the central nervous system and preferentially enriched in the mushroom bodies of the adult brain, centers for olfactory memory (Skoulakis and Davis, 1996). These studies suggest that the Leonardo protein plays an essential role in neuronal function underlying associative learning.

The *leonardo* gene encodes the *Drosophila* homolog of the  $\zeta$  isoform of the 14-3-3 protein family (Skoulakis and Davis, 1996). The 14-3-3 proteins are small, acidic, cytosolic proteins of  $\sim 30$  kDa whose crystal structure predicts dimer formation (Marais and Marshall, 1995; Jones et al., 1995; Xiao et al., 1995); each subunit consists of nine antiparallel helices, which combine to form an open, negatively charged channel. Members of the 14-3-3 family are highly conserved in a broad range of eukaryotic organisms (Aitken, 1995). In vertebrates, the family consists of seven closely related proteins (typical isoforms, 75%–92% sequence identity) and two distantly related proteins (atypical isoforms). Leonardo shows 88% amino acid identity to the mammalian 14-3-3 $\zeta$  isoform, a typical family member. Surprisingly, the multiple 14-3-3 isoforms characteristic of vertebrates seem to be absent in *Drosophila*, and Leonardo appears to be the only typical 14-3-3 protein in *Drosophila* (Skoulakis and Davis, 1996).

14-3-3 proteins have been implicated in a wide range of intracellular signaling mechanisms in many cell types (Aitken, 1995). First, 14-3-3 proteins act as regulators of protein kinase C (PKC), and have been suggested to act as both inhibitors and activators of kinase activity (Aitken et al., 1995; Xiao et al., 1995). Second, 14-3-3 proteins activate tyrosine hydroxylase (TH) and tryptophan hydroxylase (TPH), the rate-limiting enzymes in catecholamine and serotonin biosynthesis, respectively, possibly through the regulation of calmodulin kinase II (CamKII) and/or related protein kinases (Ichimura et al., 1995; Xiao et al., 1995). Third, 14-3-3 proteins interact directly with proteins of several signal transduction cascades, including CDC25 phosphatase during cell cycle control and the protein kinase RAF-1 in the mitogen-activated protein kinase (MAPK) pathway (Fantl et al., 1994; Freed et al., 1994; Irie et al., 1994; Li et al., 1995). The name "Leonardo" for the *Drosophila* 14-3-3 homolog was selected to reflect the multitude of molecular functions attributed to these proteins.

The 14-3-3 protein family is present at high concentrations in the vertebrate brain and, as elsewhere, these proteins are thought to be involved in various cellular functions, including kinase regulation and exocytosis

(Martin et al., 1994; Patel et al., 1994; Gelperin et al., 1995). In the brain, 14-3-3 proteins are found enriched in synaptic connections, where they exist in both cytosolic and synaptic vesicle bound fractions (Martin et al., 1994). Biochemical studies suggest that 14-3-3 proteins may bind  $Ca^{2+}$  (Zupan et al., 1992) and phospholipids (Roth et al., 1994). In neurosecretory cells, 14-3-3 proteins regulate secretory vesicle dynamics through modulation of the cortical actin cytoskeleton (Roth and Burgoyne, 1995). Thus, 14-3-3 proteins appear to occupy a key interface between secretory vesicles, the cytoskeleton, and regulatory kinase cascades. These observations have raised the possibility that 14-3-3 proteins regulate vesicle dynamics during synaptic transmission in the nervous system.

In this study, we have used a genetic approach to study possible 14-3-3 protein function at the synapse. We have examined the expression of the Leonardo protein at the NMJ and assayed the functional consequences of null *leonardo* mutations on synaptic transmission. We report here that Leonardo is strongly and specifically expressed in the presynaptic boutons of the NMJ. In mutants, the basic processes of synaptogenesis and excitation-secretion coupling are not perturbed, but properties of synaptic modulation such as transmission augmentation, high frequency transmission fidelity, and post-tetanic potentiation (PTP) are strongly impaired. We propose that Leonardo may function in the activity-dependent regulation of synaptic vesicle dynamics to control the pool of releasable transmitter vesicles at presynaptic fusion sites, a role that may explain its function in learning.

## Results

### Leonardo Is Expressed in Presynaptic Boutons

The *Drosophila* NMJ matures over a period of just 8 hr at 25°C during embryonic development, from initial contact between the motor neuron and its target muscle (13 hr after fertilization [AF]) to a mature synaptic arbor (21 hr AF, hatching; Broadie and Bate, 1993a; Broadie, 1994). During this process, both morphological and physiological synaptic properties are synchronously refined. Morphologically, the growth cone terminates its growth to the target muscle (12–13 hr AF), establishes the synaptic domain on the muscle (13–14 hr AF), and differentiates specialized presynaptic varicosities (15–20 hr AF), synaptic boutons, as the sites of neurotransmitter release (Broadie and Bate, 1993a; Broadie, 1994; Broadie et al., 1995). Physiologically, synaptic transmission begins soon after contact (13–14 hr AF), a functional NMJ capable of mediating muscle contraction develops (14–15 hr AF), fidelity and fatigue-resistant transmission properties mature (16–18 hr AF), and patterned, periodic synaptic transmission begins (18–20 hr AF; Broadie and Bate, 1993a, 1993b, 1993c). In the mature larvae, several distinct classes of NMJs can be classified based on bouton size, ultrastructural features, and neurotransmitter complement (type I and II with further subdivisions; Johansen et al., 1989). The mature NMJ shows features of morphological and physiological plasticity similar to those observed in other defined synaptic systems (Budnik et al., 1990; Zhong and Wu, 1991).

We assayed Leonardo protein expression in the nervous system, with an emphasis on the NMJ, using two polyclonal antisera. Both antisera are highly specific for Leonardo protein, recognize only a single spot on two-dimensional Western blots, and do not recognize an antigen in null *leonardo* mutant embryos (see below). Leonardo protein is first reliably detected in the nervous system at 16–18 hr AF in neuronal cell bodies, axons, and synapses, including the NMJ (Figure 1B). The protein is progressively partitioned to the NMJ and lost from the motor axons during the next few hours (16–20 hr AF). By 20 hr AF, Leonardo protein is tightly localized to synaptic boutons and barely detectable in axons (Figure 1B). This progression of synaptic protein localization is similar to that seen for other synaptic proteins, such as the synaptic vesicle (SV) proteins, Synaptobrevin (Sweeney et al., 1995) and Synaptotagmin (Littleton et al., 1993), and the SV-associated Cysteine String Protein (CSP; Broadie, 1996). However, Leonardo expression in the synapse is delayed relative to these other proteins; the SV proteins are first detected in the NMJ about 3 hr earlier, concurrent with the onset of synaptic transmission. Leonardo accumulates following the initial phase of synaptogenesis (16–18 hr AF), concurrent with the development of synaptic modulation properties (Broadie, 1994).

In mature larvae, Leonardo protein is highly enriched in NMJ synaptic boutons and at low levels in all surrounding tissues, including the motor axons and muscle (Figure 1C). The protein is expressed in all detectable morphological classes of NMJs, including both type I and type II (Johansen et al., 1989; Figure 1C). Double-labeling with antisera against presynaptic proteins, such as CSP (Zinsmaier et al., 1994), showed that Leonardo is expressed presynaptically and colocalizes with synaptic vesicles in the presynaptic boutons (Figure 1D). The protein is present at lower levels in axonal processes removed from the presynaptic boutons. Double-labeling experiments with antisera against postsynaptic proteins, such as the PS integrins (Broadie et al., unpublished data), show that Leonardo protein is enriched in presynaptic boutons surrounded by a halo of postsynaptic integrin protein, localized in the subsynaptic reticulum (SSR; Figure 1E). The fluorescent signal suggests that low levels of the Leonardo protein may also be present in the postsynaptic muscle.

### Null *leonardo* Mutants Are Embryonic Lethal

Mutants in *leonardo* were isolated in an enhancer detector screen for mushroom body expression; two independent and lethal P-element insertions, *leo*<sup>P1375</sup> and *leo*<sup>P1188</sup>, were recovered (Skoulakis and Davis, 1996). We have generated a series of imprecise excisions by mobilizing the P-element in *leo*<sup>P1375</sup> and from a local hop (*leo*<sup>1.3H</sup>). Two of the excision lines, *leo*<sup>12BL</sup> and *leo*<sup>7BL</sup>, have gross structural rearrangements of the *leonardo* gene as detected by Southern blotting (see Experimental Procedures). Immunohistochemical staining of *leo*<sup>12BL</sup> and *leo*<sup>7BL</sup> homozygous embryos failed to reveal significant levels of Leonardo protein. Furthermore, Western analysis of extracts from individual mutant embryos (N = 20) revealed that homozygotes for either of the alleles do

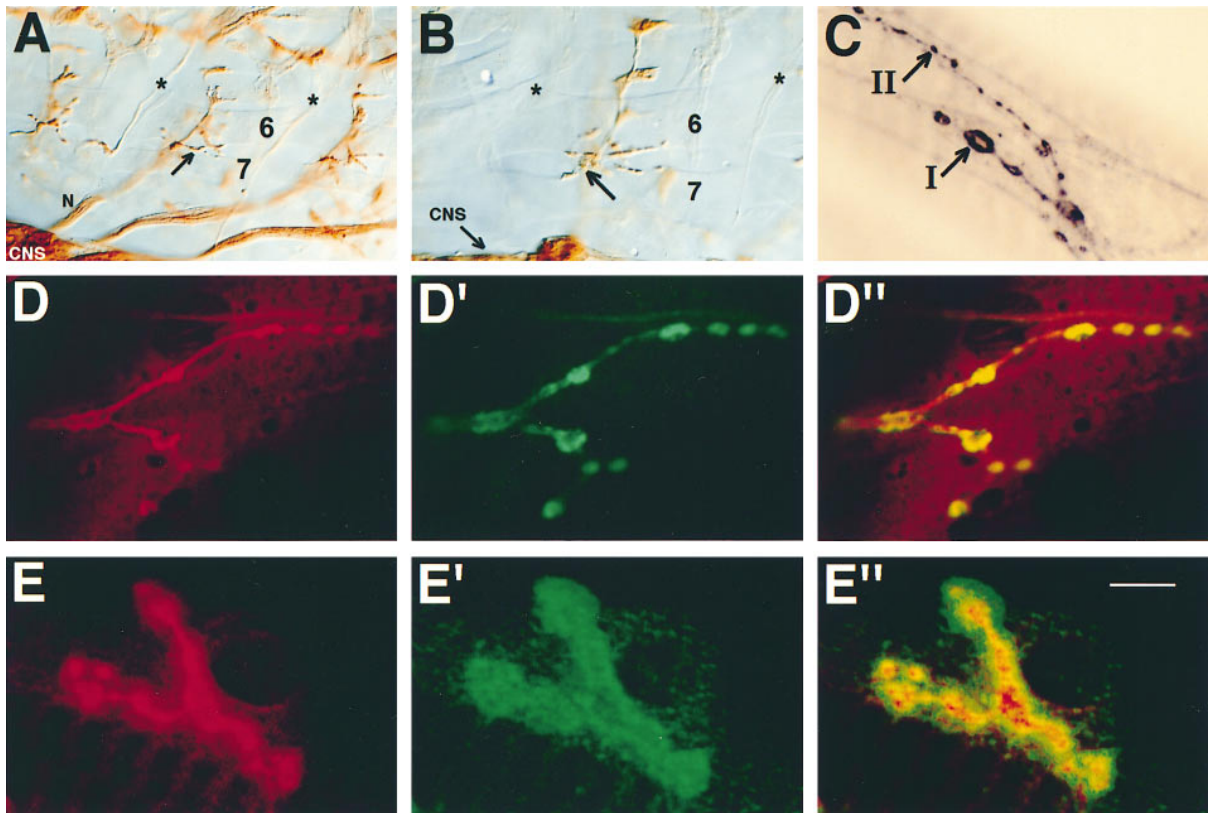


Figure 1. Leonardo Protein Is Expressed at Synaptic Contacts and Enriched in Presynaptic Boutons

(A) Null *leonardo* mutants (*leo<sup>12BL</sup>*) show a normally structured neuromusculature. The panel shows the ventral neuromusculature of three abdominal hemisegments (A2–A4) in the mature embryo (20 hr AF) stained with an antibody against Cysteine String Protein (CSP): the ventral CNS, three peripheral nerves (N), and the NMJ on muscle 6/7 (arrow). The asterisks (\*) indicate the segment boundaries. The mutant NMJ is normal in size, location, branching pattern, and bouton number.

(B) Leonardo protein expression in the wild-type embryonic NMJ (20 hr AF) revealed with an anti-Leonardo antibody. The panel shows the ventral neuromusculature of a wild-type embryo in abdominal segment A2; the arrow indicates the NMJ on muscles 6/7. The asterisks (\*) indicate the segment boundary. Leonardo protein is highly enriched in the CNS and the NMJ boutons.

(C) Leonardo protein expression in the NMJ synaptic boutons of a third instar larva. The protein is highly enriched in both type I and type II synaptic boutons.

(D–D'') A larval NMJ double-labeled for Leonardo (D, red) and the SV-associated CSP (D', green). The merged image (D'') shows the colocalization of these two proteins.

(E–E'') A larval NMJ double-labeled for Leonardo (E, red) and postsynaptic PS integrin (E', green). The merged image (E'') shows a distinct Leonardo presynaptic domain (red) surrounded by a halo of postsynaptic integrin (green).

Scale: (A) 50  $\mu$ m, (B) 30  $\mu$ m, (C–E) 10  $\mu$ m.

not contain detectable levels of Leonardo protein (Figure 2). Therefore, by these analyses, both *leo<sup>12BL</sup>* and *leo<sup>7BL</sup>* appear null for Leonardo protein expression. However, the two alleles are distinguishable by genetic complementation with the *leonardo* hypomorph *leo<sup>P1188</sup>*. The *leo<sup>12BL</sup>* allele does not complement *leo<sup>P1188</sup>* for lethality, but a few transheterozygous escapers are observed with *leo<sup>7BL</sup>*. These results suggest that *leo<sup>12BL</sup>* is a null *leonardo* allele and *leo<sup>7BL</sup>* is a very strong hypomorph.

Both *leo<sup>12BL</sup>* and *leo<sup>7BL</sup>* mutants die as mature embryos. They show a range of morphological abnormalities outside of the nervous system, including incomplete dorsal migration of the lateral epidermis and failure of dorsal epidermal closure (data not shown). However, the failure in dorsal closure appears not to be the sole cause of lethality, since the hypomorphic mutations *leo<sup>P1188</sup>* and *leo<sup>P1375</sup>* show no detectable defects in dorsal closure yet also display lethality beginning at late embryonic stages

(Skoulakis and Davis, 1996). The CNS and neuromusculature appear morphologically normal and the mutant embryos exhibit coordinated muscle movements similar to those observed in wild-type locomotion. Therefore, it is not clear whether lethality results from synaptic transmission defects (see below) or an undetected essential requirement outside of the neuromusculature.

#### Impaired Presynaptic Function at the NMJ of *leonardo* Mutants

Null *leonardo* mutants display largely normal synaptogenesis at the NMJ (Figure 1A). The muscles are innervated in the correct domain and develop presynaptic boutons similar to wild type (Figures 1A and 1B). Neither the number nor distribution of synaptic boutons in the NMJ is significantly different from normal (number of boutons at muscle 6/7 NMJ [A2]: wild type,  $17 \pm 2.8$ ; *leo<sup>7BL</sup>*,  $16 \pm 3.7$ ; *leo<sup>12BL</sup>*,  $19 \pm 3.2$ ; mean  $\pm$  SD; N = 20).

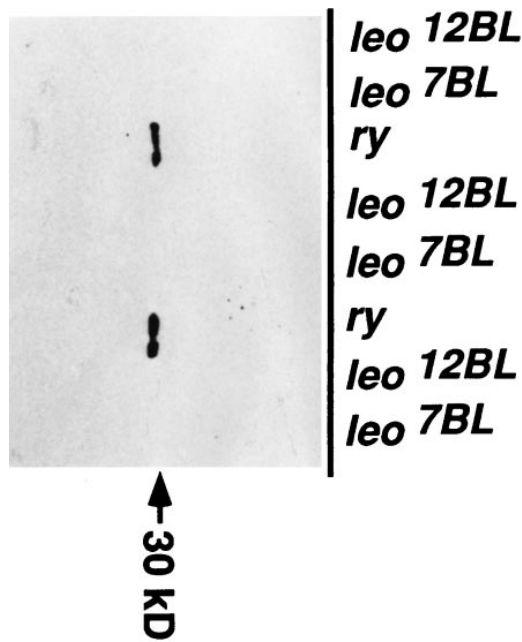


Figure 2. Absence of Leonardo Protein in Lethal *leonardo* Mutant Embryos

Mutant embryos and *ry* (*rosy*) control embryos were assayed for Leonardo protein expression at 22–23 hr AF with the anti-Leonardo antibody on Western blots. Individual embryo extracts of both genotypes (N = 20) were run in parallel. Control embryos showed a strong Leonardo band (30 kDa), whereas both mutant alleles, *leo<sup>7BL</sup>* and *leo<sup>12BL</sup>*, showed no detectable protein. Similarly, no protein expression was detected with in situ antibody labeling.

Moreover, the boutons express a normal abundance and distribution of synaptic proteins, including Synaptotagmin, Syntaxin, and CSP, as judged by immunological staining (shown for CSP in Figure 1A). All these features of morphological and molecular synaptogenesis develop with the normal timecourse, suggesting that synaptogenesis is not delayed or otherwise perturbed. Therefore, Leonardo protein does not appear to be required for morphological synaptogenesis.

The null mutant embryos also show near normal physiological development and basal excitation-secretion function at the NMJ at the end of embryogenesis (20–22 hr AF). The NMJ is functional and capable of driving robust muscle contraction (Figure 3A). As in wild type, the mutant NMJ produces rhythmic, periodic bursts of excitatory junctional currents (EJCs), which drive coordinated peristaltic muscle contractions similar to those normally observed during larval locomotion. However, the amplitude and frequency of these endogenous EJCs in *leo* mutants is significantly reduced relative to wild type (Figure 3A). This reduced function originates in a presynaptic defect, since stimulation-evoked EJC amplitude is reduced (Figure 3B), whereas the postsynaptic response to iontophoretically applied transmitter, L-glutamate, is similar to normal (Figure 3C). At a basal stimulation frequency (0.2 Hz), the mean suprathreshold peak EJC amplitude is reduced approximately 30% in the mutant compared to wild type. Thus, basal presynaptic function is mildly impaired in *leo* null mutant embryos.

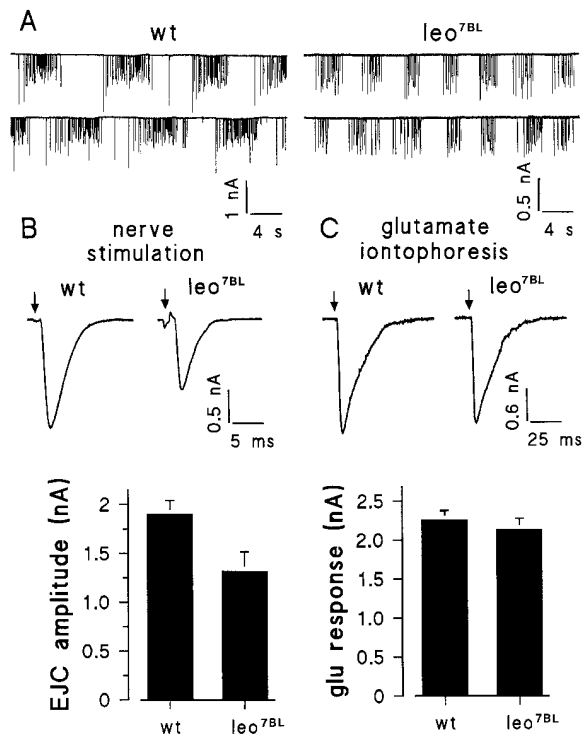


Figure 3. Null *leonardo* Mutants Display Impaired Presynaptic Function at the NMJ

(A) Endogenous synaptic currents in wild-type (*wt*) and *leo<sup>7BL</sup>* mutants recorded from the voltage-clamped (−60 mV) muscle in normal [Ca<sup>2+</sup>] (1.8 mM). Both genotypes show periodic bursts of large excitatory junction currents (EJC), which drive coordinated peristaltic movement in the body muscles.

(B) Synaptic transmission was assayed by stimulating the nerve with a suction electrode at 0.2 Hz (arrow indicates shock artifact) while recording currents in the voltage-clamped muscle. The mean peak suprathreshold EJC amplitude was measured from 10 embryos of *wt* and *leo<sup>7BL</sup>*. The mutant shows a significant 30% decrease in peak EJC amplitude. The *leo<sup>12BL</sup>* mutant shows a similar reduced amplitude of 1.26 ± 0.22 (mean ± SEM).

(C) Postsynaptic function was assayed by iontophoretic application of the transmitter, L-glutamate, to the postsynaptic membrane (arrow indicates application time) while recording current in the voltage-clamped muscle. The mean peak glutamate current amplitude was measured from 10 embryos of each *leo* genotype (shown for *leo<sup>7BL</sup>*), and no significant difference was observed with wild type. All records in this and subsequent figures were taken from muscle 6 in abdominal segment A2 of mature embryos (20–22 hr AF).

We examined the frequency and amplitude of spontaneous miniature EJCs (MEJCs) in the mutant genotypes to determine whether constitutive SV fusion is altered (Figure 4). The *Drosophila* NMJ shows two classes of MEJCs: class 1, with a larger amplitude and rapid timecourse believed to represent quantal fusion events onto the recorded muscle; and class 2, with a smaller amplitude and slower timecourse believed to represent quanta released onto adjacent, coupled muscle fibers (Broadie et al., 1995). Both classes of MEJCs are present in the *leo* mutants and show normal frequency and amplitude distributions (Figure 4A). In Ca<sup>2+</sup>-free bath, the wild-type NMJ displays a total MEJC frequency of 0.17 ± 0.06 Hz, and *leo<sup>12BL</sup>* shows a similar frequency of 0.13 ± 0.07 Hz (mean ± SEM; N = 13 and 11 cells, respectively).

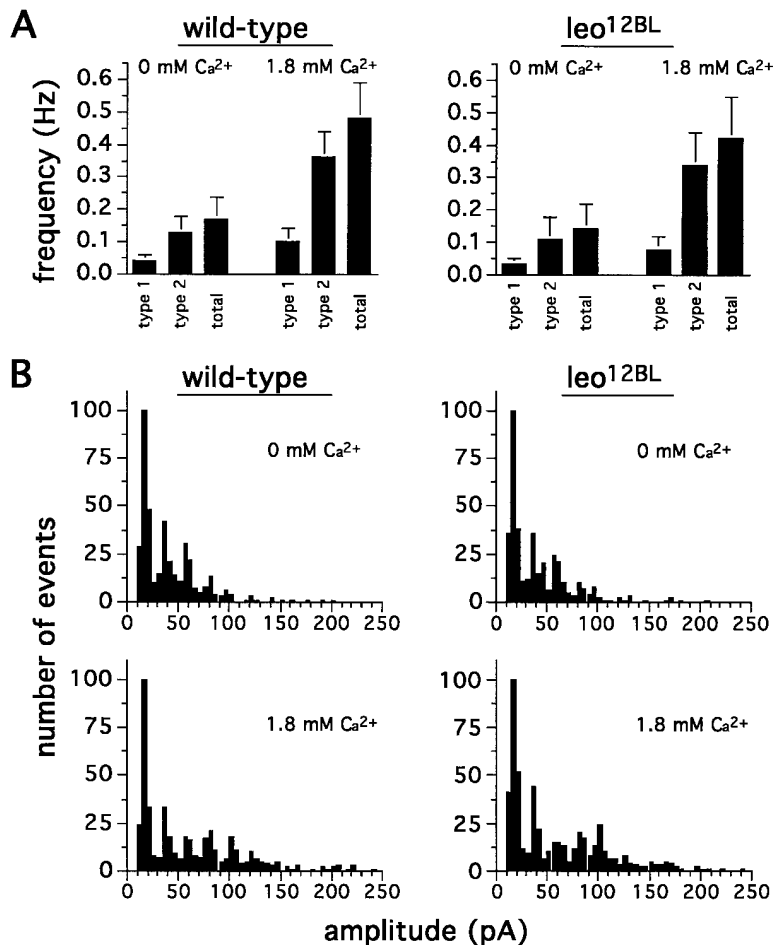


Figure 4. Miniature EJC Frequency and Amplitude Distribution Is Not Significantly Altered in *leonardo* Null Mutants

(A) The *Drosophila* NMJ shows two classes of MEJCs: class 1, larger amplitude currents with a rapid timecourse believed to represent quanta released onto the voltage-clamped muscle; and class 2, smaller amplitude currents with a slow timecourse believed to represent quanta released onto adjacent, coupled muscle fibers. Both classes of MEJCs are present in *leo*<sup>12BL</sup> at a similar frequency as in wild type. MEJC frequency was assayed both in Ca<sup>2+</sup>-free bath (0 mM Ca<sup>2+</sup>) and in standard Ca<sup>2+</sup> bath (1.8 mM Ca<sup>2+</sup>) containing 0.5 mM TTX. Each bar represents the mean  $\pm$  SEM from at least 10 embryos.

(B) The current amplitude distributions of MEJCs in wild-type and *leo*<sup>12BL</sup> embryos in 0 mM and 1.8 mM Ca<sup>2+</sup>. In each case, current amplitudes were divided into 5 pA bins, and currents were recorded until a bin collected 100 events. Both the amplitude distribution and average amplitude were similar in the two genotypes at both Ca<sup>2+</sup> concentrations.

Thus, MEJC frequency is not significantly altered in the mutant, suggesting Leonardo function specifically affects evoked transmission. The amplitude distribution of class 1 MEJCs was also similar in the null mutant and control (Figure 4B), and the average MEJC amplitude was not altered (wild type, 34.9  $\pm$  8.1 pA; *leo*<sup>12BL</sup>, 38.7  $\pm$  9.3 pA; mean  $\pm$  SEM; N = 13 and 11 cells, respectively). Thus, MEJC amplitude is not altered in the mutant, reinforcing the conclusion based on glutamate iontophoresis that glutamate receptor accumulation in the postsynaptic membrane is normal.

The evoked transmission defect in *leo* mutants is more pronounced at reduced external Ca<sup>2+</sup> concentrations. We stimulated the motor nerve with a suction electrode at 1 Hz and recorded NMJ function in a range of Ca<sup>2+</sup> levels from 0.1–1.8 mM (Figure 5A). EJC amplitude and transmission failure was quantified in wild-type and *leo* null mutants. The mutant showed a significantly depressed mean EJC transmission amplitude over the entire [Ca<sup>2+</sup>] range. At higher Ca<sup>2+</sup> levels (>1 mM Ca<sup>2+</sup>), the average EJC amplitude was reduced 50% relative to wild type, whereas at lower Ca<sup>2+</sup> levels (<0.5 mM Ca<sup>2+</sup>), the average EJC amplitude was reduced 80% or more (Figure 5A). This Ca<sup>2+</sup>-sensitive difference can be explained, at least in part, by the elevated transmission failure rate observed in the mutant at low Ca<sup>2+</sup> levels (Figure 5B). For example, in 0.2 mM Ca<sup>2+</sup>, wild-type

NMJs show a nearly 100% transmission success rate, whereas 50% of stimuli fail to elicit an EJC in the mutant. Despite these Ca<sup>2+</sup>-sensitive defects in transmission, the Ca<sup>2+</sup> cooperativity of synaptic transmission is not altered in the mutant compared to wild type, as assayed by the slope of the Ca<sup>2+</sup> dependence curves (Figure 5C). However, the Ca<sup>2+</sup> dependence curve is shifted to the right in *leo* mutants, indicating that a higher external [Ca<sup>2+</sup>] is required to achieve the given level of secretion (Figure 5C). This transmission defect in *leonardo* is similar to though less severe than that observed in *synaptotagmin* null mutants (Broadie et al., 1994).

The *leo* mutant alleles show a dorsal closure defect, which may secondarily interfere with NMJ development or function. We controlled for this possibility with two sets of controls. First, we examined a *leonardo* hypomorph (*leo*<sup>P1186</sup>), which shows no detectable dorsal closure defect, by stimulating the motor nerve with a suction electrode at 1 Hz at 0.2 and 1.0 mM external [Ca<sup>2+</sup>] and quantitating NMJ transmission amplitude and failure rate. The *leo*<sup>P1186</sup> allele showed a similar, albeit weaker, phenotype as the *leo* null. The EJC amplitudes were 0.27  $\pm$  0.11 nA and 0.94  $\pm$  0.29 nA at 0.2 and 1.0 mM Ca<sup>2+</sup>, respectively, compared with wild-type amplitudes of 0.56  $\pm$  0.05 nA and 1.63  $\pm$  0.12 nA (mean  $\pm$  SEM; N = 12 cells). Transmission failure in 0.2 mM Ca<sup>2+</sup> was 27%  $\pm$  9% in *leo*<sup>P1186</sup> compared with 4%  $\pm$  3% in

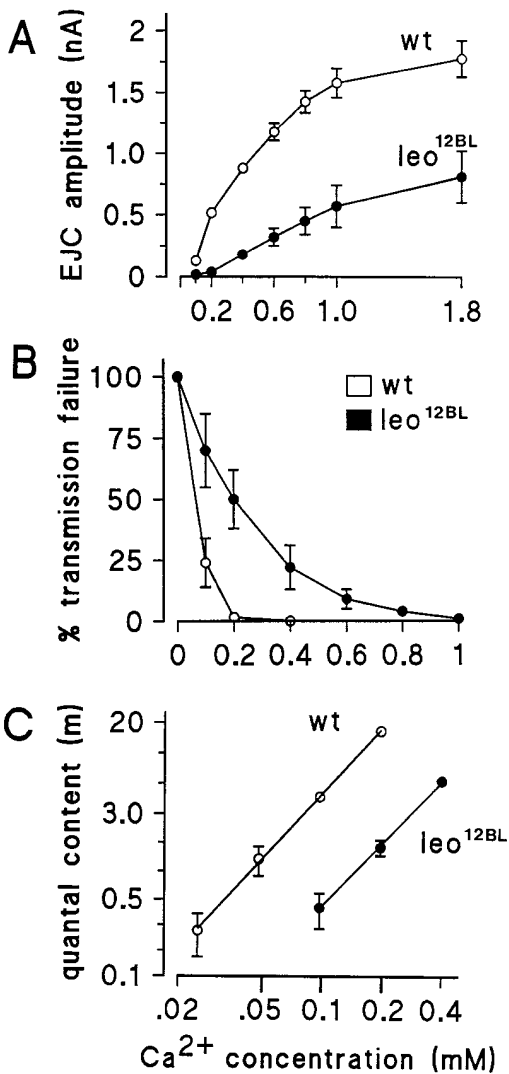


Figure 5. The Presynaptic Defect in *leonardo* Mutants Is More Severe at Low External  $Ca^{2+}$  Levels, But the  $Ca^{2+}$  Cooperativity of Transmission Is Not Altered

(A) NMJ transmission was evoked with suction-electrode stimulation of the motor nerve (1 Hz) and the mean EJC amplitude was measured in the voltage-clamped ( $-60$  mV) muscle in wild-type (wt) and *leonardo* (*leo*<sup>12BL</sup>) mutant NMJs in a range of external  $Ca^{2+}$  concentrations (0.1–1.8 mM). The *leo* mutants have significantly reduced mean EJC amplitude at all  $[Ca^{2+}]$  with the average differential increasing at lower  $[Ca^{2+}]$ .

(B) NMJ transmission failure was measured in each genotype in a range of  $[Ca^{2+}]$  (0.1–1.0 mM). At the wt NMJ, near 100% transmission success is observed in 0.2 mM  $Ca^{2+}$ . In contrast, *leo*<sup>12BL</sup> NMJs show 50% transmission failure at 0.2 mM  $Ca^{2+}$  and only approach 100% transmission success at 0.8–1.0 mM  $Ca^{2+}$ .

(C) The mean quantal content of transmission was measured in the range of 0.02–0.4 mM  $Ca^{2+}$  for each genotype. Both *leo* alleles (*leo*<sup>12BL</sup> and *leo*<sup>12BL</sup>) show the same  $Ca^{2+}$  cooperativity of quantal release as wt, as evidenced by the slopes of the two plots ( $n = 1.35$ , wt; 1.22, *leo*<sup>12BL</sup>; and 1.48, *leo*<sup>12BL</sup>), but much higher  $[Ca^{2+}]$  is required to obtain the same amount of release. Each point represents the mean  $\pm$  SEM from at least 10 embryos of each genotype.

wild type. Thus, a weak *leonardo* hypomorph, which lacks the dorsal closure defect, shows similar types of transmission dysfunction at the NMJ. Second, we

examined another dorsal closure mutant, *foreclosed* (*fc*<sup>44b</sup>), for NMJ transmission defects (Broadie and Bate, 1993a). Both the amplitude and other transmission characteristics of this mutant were not significantly different from wild type. Therefore, we conclude that the dorsal closure and synaptic transmission phenotypes are completely separable and that *leonardo* mutants show a specific defect in presynaptic function.

### Synaptic Transmission Fidelity and Fatigue Resistance Properties Are Impaired in *leonardo* Mutants

In *leonardo* mutants, synaptic transmission properties are progressively impaired with increasing stimulation frequency (Figure 6). At a basal stimulation frequency (0.2 Hz), the peak suprathreshold EJC amplitude is only mildly decreased (30%; Figure 3B), and the NMJ shows transmission fidelity and fatigue properties similar to wild type. However, at elevated stimulation frequencies (range, 1–50 Hz), transmission amplitude, fidelity, and fatigue properties are all progressively impaired (Figure 6).

Mean EJC amplitude and amplitude variation were quantified in normal  $[Ca^{2+}]$  (1.8 mM) over a range of stimulation frequencies in wild-type and *leo* null mutants. At a low stimulation frequency (1 Hz), EJC amplitude in the mutant is depressed by almost 50% relative to wild type, but the mean variability of EJC amplitude is not significantly altered (Figure 6B). At a moderate stimulation frequency (10 Hz), EJC amplitude is depressed more than 60%, and amplitude variability is doubled relative to wild type (Figure 6B). Finally, at a high stimulation frequency (50 Hz), the mutant NMJ shows an 80% depression in EJC amplitude and a 250% increase in the variability of transmission relative to a normal synapse under the same conditions (Figure 6B). These results show that the NMJ synapse in the *leo* mutant is incapable of maintaining high fidelity transmission at elevated stimulation frequencies and that the average amount of transmitter released decreases with increasing stimulation frequency.

The null mutant synapse also shows elevated transmission fatigue at high stimulation frequencies. At low to moderate stimulation frequencies (up to 10 Hz), the mutant NMJ is able to keep up with demands and shows no significant fatigue above that normally observed (Figure 6C). At 10 Hz, both wild type and mutant display a rapid 25% depression in mean EJC amplitude, which then plateaus and is maintained indefinitely. In contrast, at higher stimulation frequencies ( $>20$  Hz), the *leo* mutant NMJ displays a significantly heightened transmission fatigue relative to normal (Figure 6A). For example, at 50 Hz, the mutant EJC amplitude rapidly fatigues to 20% of its initial value, whereas the wild-type NMJ maintains transmission at  $\sim 60\%$  of its initial value (Figure 6C). In both cases, the fatigue is rapid and occurs within five stimuli in the train, after which the mean EJC value plateaus and is maintained for the duration of the train. These results show that null *leo* mutant NMJs are incapable of maintaining transmission amplitudes under conditions of high demand.

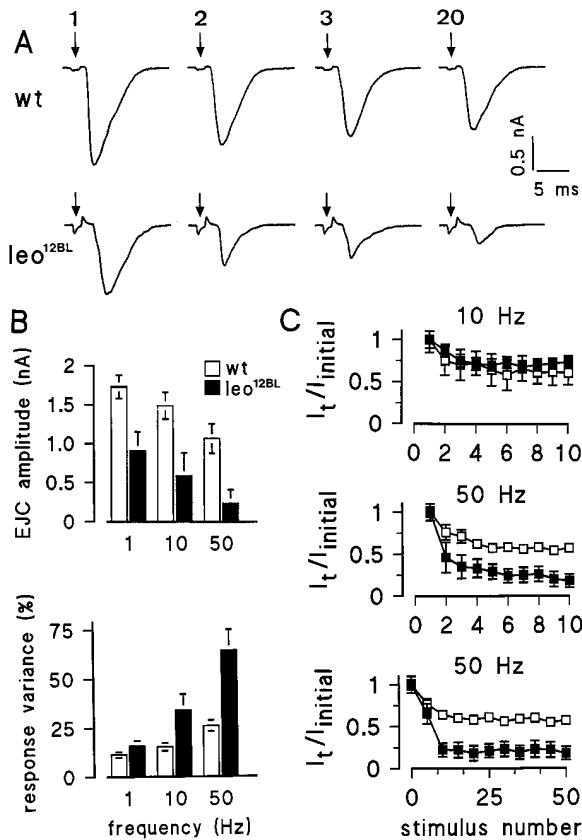


Figure 6. Synaptic Transmission Amplitude, Fidelity, and Fatigue Resistance Are Impaired in *leonardo* Mutants in a Stimulation Frequency-Dependent Manner

The NMJ was stimulated in normal  $[Ca^{2+}]$  (1.8 mM) at three frequencies, low (1 Hz), moderate (10 Hz), and high (50 Hz), and the mean EJC amplitude, EJC amplitude variance, and EJC amplitude fatigue over time were quantified. Each parameter was increasingly depressed in *leo<sup>12BL</sup>* mutants with elevated stimulation frequencies.

(A) A representative EJC record from a NMJ stimulated at 50 Hz in wt and *leo<sup>12BL</sup>*. The EJC from the first, second, third, and twentieth stimuli in the train are shown. In wt, some transmission fatigue is observed with the twentieth stimulus, producing an EJC of 60%–70% of the initial amplitude. In *leo<sup>12BL</sup>*, the initial response is only slightly reduced compared to wt, but the amplitude is rapidly depressed over the first few stimuli of the train, and the twentieth stimulus produces an EJC 20% of the initial amplitude.

(B) Mean EJC amplitude and the percent variation of EJC amplitudes in both genotypes at the three stimulation frequencies. The *leo<sup>12BL</sup>* mutant shows a more pronounced frequency-dependent depression in EJC amplitude (top plot), largely attributable to the dramatic loss of transmission fidelity (bottom plot) and fatigue at high stimulation frequencies.

(C) EJC fatigue over time is quantified as EJC amplitude ( $I_t$ ) divided by initial EJC amplitude ( $I_{initial}$ ). At moderate stimulation frequencies (10 Hz; top plot), EJC fatigue is similar in both genotypes. At high stimulation frequencies (50 Hz), the *leo<sup>12BL</sup>* mutant shows a dramatic increase in EJC fatigue, which occurs within the first few stimuli of the train (middle plot) and then is maintained for the duration of the record (bottom plot). In every plot, each point represents the mean  $\pm$  SEM from at least 10 embryos of each genotype.

**Short-Term Facilitation Is Strengthened but Synaptic Augmentation and Potentiation Are Disrupted in *leonardo* Mutants**

The *Drosophila* NMJ shows robust facilitation, augmentation, and potentiation properties (Zhong and Wu,

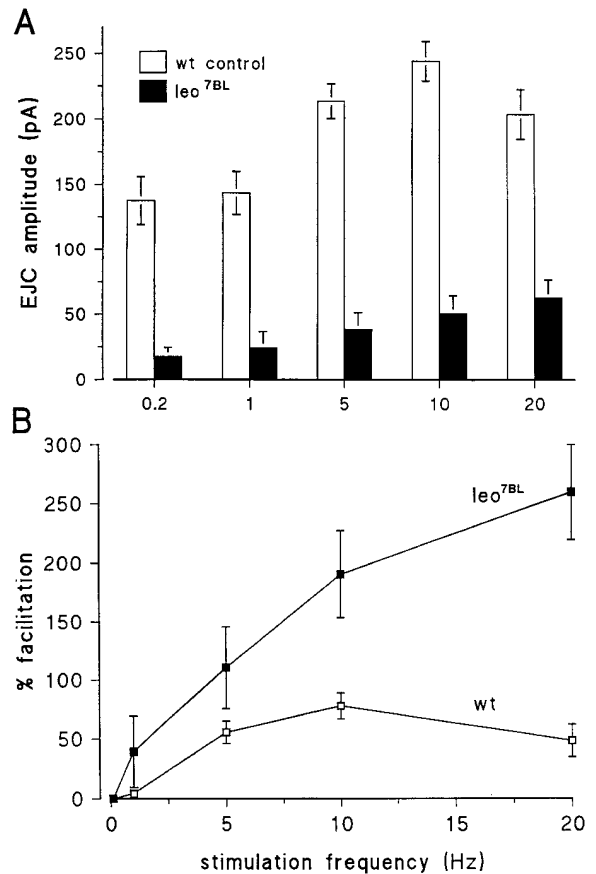


Figure 7. Short-Term Synaptic Facilitation Is Maintained in *leonardo* Mutants

The NMJ was stimulated with 20-pulse trains in the range of 0.2–20 Hz in low external  $[Ca^{2+}]$  (0.1 mM). The amplitude of the last 10 EJCs in the train was averaged (A) and divided by the initial EJC amplitude as a measure of short-term facilitation (B).

(A) Wild-type and both *leo* mutants (shown for *leo<sup>7BL</sup>*) display frequency-dependent facilitation at frequencies >1 Hz. The amplitude of the EJC events is greatly decreased in *leo* mutants relative to the control.

(B) The percent facilitation is shown over the range of stimulation frequencies. The wt NMJ shows 50% facilitation at 5–10 Hz, which then declines at higher stimulation frequencies, presumably due to the onset of fatigue. The *leo<sup>7BL</sup>* NMJ shows stronger facilitation at all stimulation frequencies, with no indication of the high frequency decline. The facilitation slope for *leo<sup>12BL</sup>* was similar to *leo<sup>7BL</sup>* (shown), with a 20 Hz facilitation of 289%  $\pm$  41% relative to the basal amplitude. Each point represents the mean  $\pm$  SEM for at least 10 embryos of each genotype.

1991). These synaptic modulation properties develop during embryonic synaptogenesis and further mature during postembryonic stages. In the mature wild-type embryo, the NMJ shows a frequency-dependent facilitation distribution with a characteristic bell shape (Figure 7). During low frequency stimulation (<1 Hz), there is modest facilitation; facilitation peaks near 100% at 5–10 Hz; and at high frequencies (>10 Hz) the NMJ begins to fatigue, and net facilitation declines. When a stimulus train is maintained, the transmission amplitude is augmented for the duration of the recording. Following a high frequency (5–10 Hz) stimulus pulse, the NMJ displays post-tetanic potentiation (PTP): EJC amplitude is

potentiated by an average of 200%, and this potentiated amplitude then decays back to baseline within a time course of several minutes (Figure 8). We examined the facilitation, augmentation, and potentiation properties of the NMJ in *leo* null mutants to determine whether these processes were affected in the absence of the protein.

Short-term facilitation was measured in low external  $[Ca^{2+}]$  (0.1 mM) by stimulating the NMJ in 20 pulse trains at increasing stimulation frequencies and dividing the mean amplitude of the last ten responses by the initial EJC amplitude (Zhong and Wu, 1991). Wild-type NMJs show significant facilitation at stimulation frequencies >3 Hz, but the degree of facilitation declines at stimulation frequencies >10 Hz, presumably due to the onset of synaptic fatigue (Figure 7). This short-term facilitation in *leo* null mutants was similar to normal. Indeed, the degree of facilitation was significantly increased in the mutant relative to normal and did not decline at stimulation frequencies >10 Hz (Figure 7). The observed elevated short-term facilitation may be due to the strongly depressed EJC amplitude observed in the mutants (Figures 5A and 7A), which may produce conditions that increase the response to facilitative integration and prevent the onset of fatigue. Based on these results, we conclude that *leo* mutants show no defect in short-term facilitation properties but rather show a substantially stronger facilitation.

We next assayed maintained transmission augmentation and PTP at the mutant synapse. The experiment involved stimulating the NMJ in low external  $[Ca^{2+}]$  (0.1 mM) at 0.5 Hz for 1 min to establish a baseline, delivering a 5 Hz stimulus train for 1 min, and then returning to a 0.5 Hz stimulation frequency for 5 more min (Figure 8A). EJC amplitudes were measured prior to the 5 Hz train, at three points during the train, and at 30 s intervals following the train (Figure 8). Under these conditions, the wild-type NMJ exhibits strong amplitude augmentation during the 5 Hz stimulus train and strong potentiation following the train (Figure 8B). The mean augmentation at the end of the 5 Hz train was 100%, followed by a mean potentiation of 200%, which then decayed over the course of 2–4 min. In the mutant, EJC amplitudes showed strong initial facilitation during the 5 Hz stimulus train (Figure 8B), similar to that observed in the short-term facilitation experiments (Figure 7B). However, this facilitation was not maintained but rather decayed over the course of the 1 min train, showing that the mutant NMJ was unable to maintain transmission augmentation (Figure 8B). Following the stimulus train, the mutant NMJ showed no indication of potentiation. Indeed, the normal PTP was replaced with a strong post-tetanic depression (PTD; Figure 8B). This PTD recovered toward the baseline value over a period of 1–2 min. These results show that while short-term facilitation is strongly apparent in the mutants, both long-term augmentation and PTP are lost in the absence of the Leonardo protein.

## Discussion

### Leonardo Is Expressed in the Presynaptic Terminal and Plays a Role in Presynaptic Function

The Leonardo protein is strongly expressed in presynaptic boutons, where it colocalizes with the transmitter

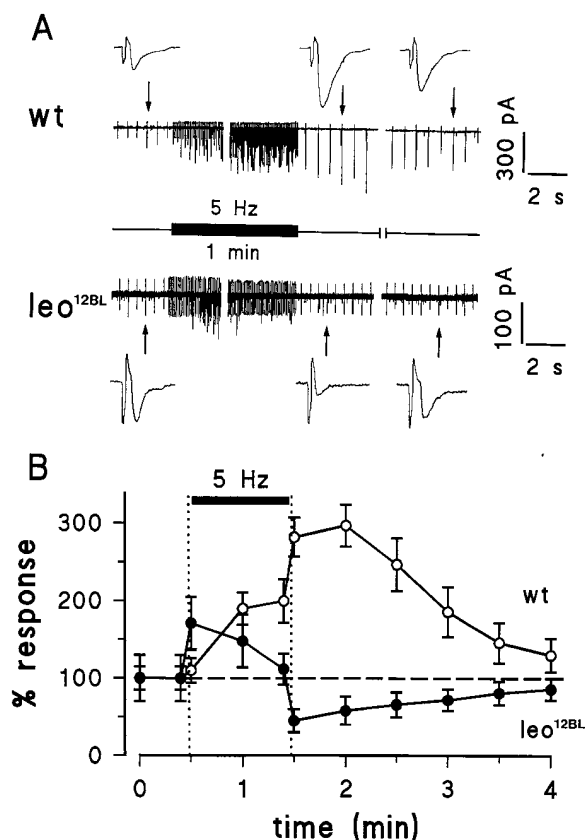


Figure 8. Post-Tetanic Potentiation (PTP) Is Replaced by Depression (PTD) in *leonardo* Mutants

To measure PTP, the NMJ was stimulated in low  $[Ca^{2+}]$  (0.1 mM) at 0.5 Hz for 1 min, given a 5 Hz stimulus train for 1 min, and then returned to the 0.5 Hz stimulation frequency. EJC amplitude was averaged prior to the 5 Hz pulse; at the beginning, middle, and end of the pulse; and at 30 s intervals following the pulse. PTP is expressed as the percentage of average EJC amplitude after the pulse over the baseline EJC average prior to the pulse.

(A) Representative traces from wt and *leo*<sup>12BL</sup> mutant. For each record, arrows indicate three EJCs, recorded prior to, immediately following, and 2 min following the 5 Hz pulse.

(B) The mean EJC response expressed as a percentage of the starting EJC amplitude. In wt, strong augmentation is observed during the 5 Hz pulse, and significant PTP is maintained for 2–3 min following the pulse. In *leo*<sup>12BL</sup>, initial facilitation is observed during the 5 Hz pulse followed by a decay in augmentation. Following the pulse, the *leo*<sup>12BL</sup> NMJ shows significant PTD, which returns to baseline over the course of a few minutes. The *leo*<sup>7BL</sup> mutant (not shown) shows a similar PTD phenotype with a amplitude depression of  $44\% \pm 11\%$  at the first time point following the stimulus. Each point represents the mean  $\pm$  SEM from at least 10 records made from at least 5 embryos of each genotype.

vesicle population. The onset of Leonardo expression in the embryonic NMJ is coincident with the development of synaptic modulation properties (facilitation, augmentation, and potentiation), which follow the initial stages of synaptogenesis (target recognition, synapse morphogenesis, excitation-secretion coupling). This expression pattern is consistent with the possibility that Leonardo may participate in late-developing mechanisms of synaptic modulation through interaction with synaptic vesicles. It is possible that Leonardo plays a

specific role in the development of presynaptic properties at the NMJ. For example, the protein may be involved in the maturation of presynaptic terminals to allow high frequency, high fidelity release of synaptic vesicles. However, the maintenance of high level protein expression at the mature larval NMJ, and the absence of any detectable defects in molecular or morphological synaptic development, suggest that Leonardo plays a sustained role in synaptic function.

Null *leonardo* mutants are embryonic lethal and show defects in presynaptic function. The basic process of neurotransmission appears largely normal, since the NMJ is capable of mediating patterned synaptic communication to drive coordinated movement. However, basal NMJ excitation-secretion coupling is reduced by 30% relative to normal. This presynaptic transmission defect is heightened by lowered external  $[Ca^{2+}]$  and elevated stimulation frequencies, both of which result in a strong depression of synaptic current amplitude, transmission fidelity, and fatigue resistance properties. Moreover, while short-term facilitation is robust in the mutant, long-term transmission augmentation and post-tetanic potentiation are both lost. Indeed, the mutant NMJ shows a period of transmission depression following high frequency stimulus trains. These observations show that Leonardo plays an important role in presynaptic function.

The results of this study are consistent with the hypothesis that Leonardo regulates the pool of fusion-competent vesicles in the *Drosophila* NMJ. Our observations suggest that the basic trafficking and presynaptic availability of vesicles does not require Leonardo. However, under conditions of high vesicle demand, transmission begins to fail. Thus, the mutant phenotypes are consistent with a defect in the mobilization or recruitment of vesicles to the presynaptic fusion sites. Since lowered external  $[Ca^{2+}]$  also increases mutant dysfunction, it is possible that Leonardo acts in the chain linking activity-dependent  $Ca^{2+}$  influx to the mobilization or utilization of the presynaptic vesicle pool. This hypothesis is consistent with the protein expression pattern and offers a plausible explanation for the learning defect in *leonardo* mutants (Skoulakis and Davis, 1996).

#### 14-3-3 Proteins and Synaptic Function

Leonardo is a typical member of the 14-3-3 protein family, which shows 88% amino acid identity to its closest mammalian homolog, 14-3-3 $\zeta$  (Skoulakis and Davis, 1996). The 14-3-3 proteins have been implicated in a wide range of physiological processes involving conserved signal transduction cascades, but no family member has ever before been directly linked to the mechanisms of presynaptic function. However, three existing sets of data support the results of this study and suggest that 14-3-3 proteins may be involved in presynaptic function in a range of species. First, 14-3-3 proteins were initially identified as abundant proteins in the mammalian and avian brain (Patel et al., 1994) and are strongly expressed in neuronal synapse fractions (Martin et al., 1994). Second, it is known that 14-3-3 proteins exist in both cytosolic and membrane-associated fractions (Martin et al., 1994; Roth et al., 1994).

Biochemical work has suggested that these proteins are directly bound to the plasma membrane of synaptic vesicles in the mammalian brain (Martin et al., 1994). Third, in vitro assays have shown that 14-3-3 proteins can directly bind phospholipids and may bind  $Ca^{2+}$  (Zupan et al., 1992; Roth et al., 1994). Taken together, these studies are consistent with a role for 14-3-3 proteins in regulating synaptic vesicle dynamics.

Two related model systems give insight into the possible mechanisms of 14-3-3 synaptic function. First, in yeast, 14-3-3 proteins function in vesicle trafficking between the Golgi and plasma membrane (Gelperin et al., 1995). It is possible that this role has relevance to 14-3-3 function at the synapse, since many vesicle pathway proteins have conserved functions from yeast to neurons (Bennett and Scheller, 1993). In particular, Syntaxin and Rop, a *Drosophila* homolog of yeast SEC1, appear to have presynaptic functions at the *Drosophila* NMJ consistent with the function of their yeast homologs (Broadie et al., 1995; Schulze et al., 1995). Second, catecholamine secretion from bovine adrenal chromaffin cells is strongly potentiated by application of exogenous 14-3-3 proteins (Roth et al., 1994; Roth and Burgoyne, 1995; Chamberlain et al., 1995). The activation of  $Ca^{2+}$ -dependent secretion by 14-3-3 proteins occurs in the ATP-dependent priming step in the pathway. The 14-3-3 proteins appear to potentiate neurosecretion by causing a reorganization of the cortical actin cytoskeleton to increase vesicle access to the plasma membrane and enlarge the readily releasable pool of secretory vesicles (Roth and Burgoyne, 1995). Since many mechanisms of neurosecretion and synaptic transmission are highly conserved, it is tempting to speculate that Leonardo may also mediate its presynaptic role by regulating the actin cytoskeleton in order to control availability of transmitter vesicles at presynaptic active sites.

#### 14-3-3 Proteins and Signal Transduction Cascades

How might 14-3-3 proteins be involved in regulating the synaptic cytoskeleton and the presynaptic availability of neurotransmitter vesicles? The 14-3-3 protein family modulates a number of signal transduction cascades in a wide variety of cell types. Of potential importance at the synapse is the regulation of protein kinase A (PKA), protein kinase C (PKC), and the protein kinase RAF-1 (Fantl et al., 1994; Freed et al., 1994; Irie et al., 1994; Li et al., 1995). Functional plasticity at the synapse is influenced by overlapping cassettes of these signal transduction cascades, whose function depends on the previous activity history of the synapse. The mechanisms behind these plastic changes probably include regulation of vesicle mobilization, control of release probability at independent active sites, and the modulation of other steps in exocytotic release. The role of overlapping signaling kinases has been observed in systems ranging from sensory neuron synapses in *Aplysia* to mammalian hippocampal synapses (Nicoll and Malenka, 1995; Capogna et al., 1995). For example, PKA and PKC have been shown to have overlapping roles in synaptic facilitation in *Aplysia*, with PKA dominating in short-term facilitation, PKC in long-term facilitation, and both together contributing to intermediate forms (Byrne

and Kandel, 1996). Moreover, the effect of 14-3-3 proteins in triggering  $\text{Ca}^{2+}$ -dependent neurosecretion from bovine adrenal cells is strongly potentiated by the co-activation of PKC (Chamberlain et al., 1995). Elegant work using membrane capacitance measurements has shown that PKC acts to increase the pool size of readily releasable secretory vesicles without a major change in the  $\text{Ca}^{2+}$  dependence of exocytosis (Gillis et al., 1996). We favor the hypothesis that Leonardo interacts with PKC or related kinases in a similar synaptic pathway to regulate the size of the readily releasable vesicle pool at presynaptic active sites.

An alternative hypothesis is that presynaptic kinases regulate exocytosis through the direct modulation of the fusion machinery. Many components of the presynaptic release machinery (e.g.,  $\text{Ca}^{2+}$  channels, Syntaxin, Rab3, Synaptobrevin, etc.) are known to be phosphorylated by various kinases (Greengard et al., 1993; Nielander et al., 1995), and it has been suggested that these kinases function to modulate directly vesicle release probability downstream of  $\text{Ca}^{2+}$  influx (Trudeau et al., 1996). Activation of the PKC and PKA pathways may facilitate synaptic transmission through this presynaptic mechanism (Weisskopf et al., 1994; Capogna et al., 1995). For example, inhibition of PKA in hippocampal neurons blocks synaptic facilitation, apparently by regulating the probability of exocytosis of individual vesicles (Trudeau et al., 1996). Interaction of Leonardo with protein kinases in this pathway is also consistent with many of the observations of this study. Thus, Leonardo may be directly interacting with presynaptic kinases to regulate the phosphorylation and functional characteristics of the vesicle release machinery.

Taken together, these studies suggest that Leonardo may be interacting with one or more presynaptic kinases to regulate the pool of readily releasable synaptic vesicles in the *Drosophila* NMJ. The best studied transduction cascade at the *Drosophila* NMJ is the cAMP second messenger system (Davis, 1996). Mutations in *dunce*, which increase cAMP concentration, or *rutabaga*, which decrease cAMP, both cause impaired synaptic facilitation and PTP. This effect has been explained, in part, through the cAMP-dependent modulation of  $\text{K}^+$  currents, broadening spike duration and influencing  $\text{Ca}^{2+}$  entry (Zhong and Wu, 1993). However, it also appears that there are distinct impacts of cAMP on short-term facilitation and potentiation, probably mediated through PKA (i.e., *DCO*) and related kinases. CaM kinase also plays a role in the synaptic facilitation and potentiation and in the maintenance of synaptic fidelity at the *Drosophila* NMJ (Wang et al., 1994). Finally, PACAP-like neuropeptide transmission coactivates the cAMP and RAS/RAF MAP kinase pathways to modulate both synaptic and  $\text{K}^+$  currents at the *Drosophila* NMJ (Zhong, 1995). The loss of elements in these signaling cascades, particularly the cAMP and CaM kinase pathways, result in presynaptic defects strikingly similar to those observed in *leonardo* mutants. A priority for future research will be to establish whether one or more of these pathways directly interact with Leonardo to regulate presynaptic function.

## Experimental Procedures

### *Drosophila* Stocks

The *leo*<sup>P1188</sup>/*CyO*; *ry*<sup>506</sup> and *leo*<sup>P1375</sup>/*CyO*; *ry*<sup>506</sup> lines were isolated in an enhancer detector screen for genes preferentially expressed in the mushroom bodies. Both strains contain noncomplementary lethal insertions in the first intron of the *leonardo* gene. Mobilization of the *leo*<sup>P1375</sup> P-element yielded viable excision alleles and one viable hop (*leo*<sup>P1.3H</sup>) in the second intron of the gene (Skoulakis and Davis, 1996). An additional lethal allele (*leo*<sup>7BL</sup>) was isolated during the *leo*<sup>P1375</sup> P-element mobilization. The *leo*<sup>12BL</sup> allele was independently generated by mobilization of the viable insertion in intron two mentioned above. Molecularly, *leo*<sup>12BL</sup> harbors two partially deleted enhancer detector transposons. One is in the first intron, proximal to the P-element in *leo*<sup>P1188</sup>, and is associated with additional genomic rearrangements in that region that result in a 2 kb increase in the size of the intron. The second deleted transposon resides in the original location of the parental *leo*<sup>P1.3H</sup>. Allele *leo*<sup>7BL</sup> retains a partially deleted P-element in the site of the original *leo*<sup>P1375</sup> in addition to a 500 bp deletion in intron two. Western analysis of single *leo*<sup>7BL</sup> or *leo*<sup>12BL</sup> mutant embryos selected at 22–24 hr AF on the basis of the morphological phenotype failed to detect appreciable amounts of Leonardo protein (see below). The *leo*<sup>12BL</sup> allele is considered a null *leonardo* mutant based on the molecular characterization of the mutant gene, the absence of detectable Leonardo protein in homozygous mutant embryos, and the failure to complement the lethality of a *leonardo* hypomorph (*leo*<sup>P1188</sup>). The *leo*<sup>7BL</sup> allele is considered a strong hypomorphic mutant based on a low percentage of progeny surviving from a cross with *leo*<sup>P1188</sup>.

Fly stocks were raised on standard cornmeal food at 25°C. The *leonardo* mutants were outcrossed to the wild-type strain OR-R, and the mutant genotype was determined by failure to hatch at 22 hr AF and failure of epidermal dorsal closure. The wild-type strain OR-R was used for all control measurements. All phenotypes were confirmed by crossing the mutant lines to a balancer containing a lacZ reporter gene construct and assaying the absence of reporter gene expression with X-gal incubation following the recording session. As a control for the dorsal closure phenotype in null *leonardo* mutants, we examined another mutant with a severe dorsal closure defect called *foreclosed* (*fc*<sup>P44db</sup>), as reported previously (Broadie and Bate, 1993a).

### Histology and Western Blot Analysis

Two rabbit polyclonal anti-Leonardo antibodies were generated and characterized as described previously (Skoulakis and Davis, 1996). Both antisera contained high titers of anti-Leonardo antibody and showed high specificity binding the single Leonardo band on Western blots, both as crude antisera and following affinity purification of the antibodies (Skoulakis and Davis, 1996). The antisera show high recognition for the Leonardo protein in situ in the adult brain, and specific staining was absent in the null *leonardo* mutant embryos. Leonardo protein expression in lethal mutant embryos was assayed on Western blots using the anti-Leonardo antibodies. Embryos were collected from a balanced population for 1 hr and aged to 22–23 hr AF at 23°C. Following dechorionization and removal of the vitelline membrane, individual embryos were homogenized in 20 ml Laemli buffer, and the extracts were run on 14% acrylamide gels and probed with the anti-Leonardo antibody (1:7000). The results were visualized with a horseradish peroxidase conjugated secondary antibody and enhanced chemiluminescence (SuperSignal, Pierce).

*Drosophila* embryos and larvae were immunohistologically stained as reported previously (Broadie and Bate, 1993a; Broadie et al., 1995). Staged animals were dissected along the dorsal midline, pinned open, and fixed for 30–60 min with 4% paraformaldehyde in phosphate buffered saline (PBS; 0.02 M phosphate buffer, 0.1 M NaCl [pH 7]). Following fixation, the preparations were washed repetitively in PBT (0.1% Triton X-100 in PBS), which then formed the base solution for the remaining staining trials. To examine Leonardo expression, preparations were probed with the rabbit polyclonal anti-Leonardo antibody at a dilution in the range of 1:100 (confocal fluorescence) or 1:2000 (DAB reaction) in PBT. To examine NMJ

morphology and synaptic protein domains, preparations were probed with the following: a mouse monoclonal anti-Cysteine String Protein antibody (1:10; Zinsmaier et al., 1994; kindly provided by K. Zinsmaier), a rabbit polyclonal anti-Synaptotagmin antibody (1:1000; Littleton et al., 1993; kindly provided by H. Bellen), and a mouse monoclonal anti- $\beta$ PS-integrin antibody (1:500; CF6G11; kindly provided by N. Brown). All preparations were probed with the appropriate biotinylated secondary antibody (Vectastain) at 1:200 dilution in PBT.

Two visualization procedures were used in this study. First, staining was visualized using a Vectastain ABC Elite kit with DAB reaction and  $\text{NiCl}_2$  enhancement as reported previously (Broadie and Bate, 1993a; Broadie et al., 1995). After staining, the preparations were dehydrated using an ethanol series, cleared in HistoClear, and mounted in DPX for observation with a Zeiss Axiophot microscope. Second, staining was visualized with an avidin-conjugated fluorochrome, and the preparation was mounted in glycerol. Preparations were viewed on a confocal microscope, and optical sections of the neuromusculature were collected for analysis. Presentation figures were constructed using Adobe Photoshop software.

#### Whole-Cell Patch-Clamp Physiology

Electrophysiology was performed on the identified NMJ on muscle 6 in the anterior abdomen (A2–A3) of mature embryos (20–24 hr AF) as reported previously (Broadie and Bate, 1993a, 1993b, 1993c; Broadie et al., 1995). Whole-cell recordings from the muscle were made using standard patch-clamp techniques, using both voltage-clamp (–60 mV) and current-clamp configurations. The motor nerve was stimulated with a fire-polished suction electrode (range 2–5 V; 1 ms) to drive NMJ transmission as reported previously (Broadie and Bate, 1993a; Broadie et al., 1995). Postsynaptic function was assayed by applying transmitter, L-glutamate (1.0 mM [pH 8.0]; Sigma), directly to the postsynaptic muscle membrane with an iontophoretic pipette (resistance, 20 M $\Omega$ ) positioned <1  $\mu\text{m}$  from the Nomarski-visualized NMJ. The glutamate was applied with short pulses (1 ms) of negative current as reported previously (Broadie and Bate, 1993a). All records were made in normal fly saline (Broadie and Bate, 1993a) containing 1.8 mM  $\text{Ca}^{2+}$ , unless otherwise indicated. Signals were amplified using an Axon Instrument Axopatch-1D amplifier and filtered at 2 kHz. Data were statistically analyzed using pCLAMP 5.1 software (Axon Instruments).

Quantal content (m) was determined by dividing the evoked EJC amplitude by the quantal amplitude, quantified by measurement of spontaneous MEJC amplitudes and evoked quantal amplitudes in low external  $\text{Ca}^{2+}$  (Broadie et al., 1994; Broadie et al., 1995). The mean amplitude from these two quantal amplitude measurements is not significantly different. Failures are very clearly separable from single quantal events in the whole-cell recording configuration.

#### Facilitation and Potentiation Records

Facilitation and potentiation were assayed in low external  $\text{Ca}^{2+}$  (0.1 mM), since these synaptic properties were obscured by transmission fatigue at higher  $\text{Ca}^{2+}$  levels. Short-term facilitation was assayed by delivering 20-stimuli trains at a range of frequencies (0.2–20 Hz) and comparing the mean EJC amplitude of the last 10 responses to the starting EJC amplitude, as reported previously by Zhong and Wu (1991). Long-term augmentation was assayed using a similar paradigm, with the stimulus train lasting 1 min or longer. Post-tetanic potentiation (PTP) was assayed by delivering a 5 Hz stimulus train for 1 min and comparing the mean EJC amplitude prior to and following the high frequency stimulus, as reported previously by Zhong and Wu (1991). The mean EJC amplitude at all time points was determined by averaging the 10 EJC responses immediately surrounding the time point. Measurement were taken prior to the stimulus train; at the beginning, middle, and end of the stimulus train; immediately following the train; and at 30 s intervals thereafter.

#### Acknowledgments

We are grateful to H. Bellen, N. Brown, and K. Zinsmaier for kindly providing antibodies. We thank M. Bate, in whose lab these studies were initiated, and E. King for advice on the confocal microscope.

E. M. C. S was supported by National Research Award GM15406. R. L. D. was supported by the National Institutes of Health, Mathers Charitable Trust, and R. P. Doherty Welch Chair in Science. K. B. was supported by a Young Investigator Award from the Office of Naval Research and an Alfred P. Sloan Fellowship.

Received March 17, 1997; revised July 7, 1997.

#### References

- Aitken, A. (1995). 14-3-3 proteins on the MAP. *Trends Biochem. Sci.* **20**, 95–97.
- Aitken, A., Howell, S., Jones, D., Madrazo, J., Marin, H., Patel, Y., and Robinson, K. (1995). Post-translationally modified 14-3-3 isoforms and inhibition of protein kinase C. *Mol. Cell Biochem.* **149**, 41–49.
- Bennett, M.K., and Scheller, R.H. (1993). The molecular machinery for secretion is conserved from yeast to neurons. *Proc. Natl. Acad. Sci. USA* **90**, 2559–2563.
- Broadie, K. (1994). Synaptogenesis in *Drosophila*: coupling genetics and electrophysiology. *J. Physiol.* **88**, 123–139.
- Broadie, K. (1996). Regulation of the synaptic vesicle cycle in *Drosophila*. *Biochem. Soc. Trans.* **24**, 639–645.
- Broadie, K., and Bate, M. (1993a). Development of the embryonic neuromuscular synapse of *Drosophila melanogaster*. *J. Neurosci.* **13**, 144–166.
- Broadie, K., and Bate, M. (1993b). Innervation directs receptor synthesis and localization in *Drosophila* embryo synaptogenesis. *Nature* **361**, 350–353.
- Broadie, K., and Bate, M. (1993c). Activity-dependent development of the neuromuscular synapse during *Drosophila* embryogenesis. *Neuron* **11**, 607–619.
- Broadie, K., Bellen, H.J., DiAntonio, A., Littleton, J.T., and Schwarz, T.L. (1994). The absence of Synaptotagmin disrupts excitation-secretion coupling during synaptic transmission. *Proc. Natl. Acad. Sci. USA* **91**, 10727–10731.
- Broadie, K., Prokop, A., Bellen, H.J., O’Kane, C.J., Schulze, K.L., and Sweeney, S.T. (1995). Syntaxin and Synaptobrevin function downstream of vesicle docking in *Drosophila*. *Neuron* **15**, 663–673.
- Budnik, V., Zhong, Y., and Wu, C.-F. (1990). Morphological plasticity of motor axon terminals in *Drosophila* mutant with altered excitability. *J. Neurosci.* **10**, 3754–3768.
- Byers, D., Davis, R.L., and Kiger, J.A. (1981). Defect in cyclic AMP phosphodiesterase due to the *dunce* mutation of learning in *Drosophila melanogaster*. *Nature* **289**, 79–81.
- Byrne, J.H., and Kandel, E.R. (1996). Presynaptic facilitation revisited: state and time dependence. *J. Neurosci.* **16**, 425–435.
- Capogna, M., Gähwiler, B.H., and Thompson, S.M. (1995). Presynaptic enhancement of inhibitory synaptic transmission by protein kinase A and C in the rat hippocampus in vitro. *J. Neurosci.* **15**, 1249–1260.
- Chamberlain, L.H., Roth, D., Morgan, A., and Burgoyne, R.D. (1995). Distinct effects of  $\alpha$ -SNAP, 14-3-3 proteins, and calmodulin on priming and triggering of regulated exocytosis. *J. Cell Biol.* **130**, 1063–1070.
- Davis, R. (1996). Physiology and biochemistry of *Drosophila* learning mutants. *Physiol. Rev.* **76**, 299–317.
- Drain, P., Polkers, E., and Quinn, W.G. (1991). cAMP-dependent protein kinase and the disruption of learning in transgenic flies. *Neuron* **6**, 71–82.
- Fantl, W.J., Muslin, A.J., Kikuchi, A., Martin, J.A., MacNicol, A.M., Gross, R.W., and Williams, L.T. (1994). Activation of Raf-1 by 14-3-3 proteins. *Nature* **371**, 612–614.
- Freed, E., Symons, M., Macdonald, S.G., McCormick, F., and Ruggieri, R. (1994). Binding of 14-3-3 proteins to the protein kinase Raf and effects on its activation. *Science* **265**, 1713–1716.
- Gelperin, D., Weigle, J., Nelson, K., Roseboom, P., Irie, K., Matsumoto, K., and Lemmon, S. (1995). 14-3-3 proteins: potential roles in

- vesicular transport and Ras signaling in *Saccharomyces cerevisiae*. *Proc. Natl. Acad. Sci. USA* 92, 11539–11543.
- Gillis, K.D., Mobner, R., and Neher, E. (1996). Protein Kinase C enhances exocytosis from chromaffin cells by increasing the size of the readily releasable pool of secretory granules. *Neuron* 16, 1209–1220.
- Greengard, P., Valtorta, F., Czernik, A.J., and Benfenati, F. (1993). Synaptic vesicle phosphoproteins and regulation of synaptic function. *Science* 259, 780–785.
- Ichimura, T., Uchiyama, J., Kunihiro, O., Ito, M., Horigome, T., Omata, S., Shinkai, F., Kaji, H., and Isobe, T. (1995). Identification of the site of interaction of the 14-3-3 protein with phosphorylated tryptophan hydroxylase. *J. Biol. Chem.* 270, 28515–28518.
- Irie, K., Gotoh, Y., Yashar, B.M., Errede, B., Nishida, E., and Matsumoto, K. (1994). Stimulatory effects of yeast and mammalian 14-3-3 proteins on the Raf protein kinase. *Science* 265, 1716–1719.
- Johansen, J., Halpern, M.E., Johansen, K., and Keshishian, H. (1989). Stereotypic morphology of glutamatergic synapses on identified muscle cells of *Drosophila* larvae. *J. Neurosci.* 9, 710–725.
- Jones, D.H., Ley, S., and Aitken, A. (1995). Isoforms of 14-3-3 protein can form homo- and heterodimers in vivo and in vitro: implications for function as adapter proteins. *FEBS Lett.* 368, 55–58.
- Levin, I.R., Han, P.-L., Hwang, P.M., Feinstein, P.G., Davis, R.L., and Reed, R.R. (1992). The *Drosophila* learning and memory gene *rutabaga* encodes a Ca<sup>2+</sup>/calmodulin-responsive adenylyl cyclase. *Cell* 68, 479–489.
- Li, S., Janosch, P., Tanji, M., Rosenfeld, G.C., Waymire, J.C., Mischak, H., Kolch, W., and Sedivy, J.M. (1995). Regulation of Raf-1 kinase activity by the 14-3-3 family of proteins. *EMBO J.* 14, 685–696.
- Littleton, J.T., Bellen, H.J., and Perin, M.S. (1993). Expression of synaptotagmin in *Drosophila* reveals transport and localization of synaptic vesicles in the synapse. *Development* 118, 1077–1088.
- Marais, R., and Marshall, C. (1995). 14-3-3 proteins: structure resolved, functions less clear. *Structure* 3, 751–753.
- Martin, H., Rostas, J., Patel, Y., and Aitken, A. (1994). Subcellular localization of 14-3-3 isoforms in rat brain using specific antibodies. *J. Neurochem.* 63, 2259–2265.
- Nicoll, R.A., and Malenka, R.C. (1995). Contrasting two forms of LTP in the hippocampus. *Nature* 377, 115–118.
- Nielander, H.B., Onofri, F., Valtorta, F., Schiavo, G., Montecucco, C., Greengard, P., and Benfenati, F. (1995). Phosphorylation of VAMP/synaptobrevin in synaptic vesicles by endogenous protein kinases. *J. Neurochem.* 65, 1712–1720.
- Patel, Y., Martin, H., Howell, S., Jones, D., Robinson, K., and Aitken, A. (1994). Purification of 14-3-3 protein and analysis of isoforms in chicken brain. *Biochem. Biophys. Acta.* 1222, 405–409.
- Roth, D., and Burgoyne, R.D. (1995). Stimulation of catecholamine secretion from adrenal chromaffin cells by 14-3-3 proteins is due to reorganization of the cortical actin network. *FEBS Lett.* 374, 77–81.
- Roth, D., Morgan, A., Martin, H., Jones, D., Martens, G.J., Aitken, A., and Burgoyne, R.D. (1994). Characterization of 14-3-3 proteins in adrenal chromaffin cells and demonstration of isoform specific phospholipid binding. *Biochem. J.* 301, 305–310.
- Schulze, K.L., Broadie, K., Perin, M.S., and Bellen, H.J. (1995). Genetic and electrophysiological studies of *Drosophila* syntaxin-1A demonstrate its role in nonneuronal secretion and its essential role in neurotransmitter release. *Cell* 80, 311–320.
- Skoulakis, E.M.C., and Davis, R.L. (1996). Olfactory learning deficits in mutants for *leonardo*, a *Drosophila* gene encoding a 14-3-3 protein. *Neuron* 17, 931–944.
- Sweeney, S.T., Broadie, K., Keane, J., Niemann, H., and O’Kane, C.J. (1995). Targeted expression of tetanus toxin light chain in *Drosophila* specifically eliminates synaptic transmission and causes behavioral defects. *Neuron* 14, 341–351.
- Trudeau, L.-E., Emery, D.G., and Haydon, P.G. (1996). Direct modulation of the secretory machinery underlies PKA-dependent synaptic facilitation in hippocampal neurons. *Neuron* 17, 789–797.
- Wang, J., Renger, J.J., Griffith, L.C., Greenspan, R.J., and Wu, C.-F. (1994). Concomitant alterations of physiological and developmental plasticity in *Drosophila* CaM Kinase II-inhibited synapses. *Neuron* 13, 1373–1384.
- Weisskopf, M.G., Castillo, P.E., Zalutsky, R.A., and Nicoll, R.A. (1994). Mediation of hippocampal mossy fiber long-term potentiation by cyclic AMP. *Science* 265, 1878–1882.
- Xiao, B., Smerdon, S.J., Jones, D.H., Dodson, G.G., Soneji, Y., Aitken, A., and Gamblin, S.J. (1995). Structure of a 14-3-3 protein and implications for coordination of multiple signaling pathways. *Nature* 376, 188–191.
- Yin, J.C., Wallach, J.S., Del Vecchio, M., Wilder, E.L., Zhou, H., Quinn, W.G., and Tully, T. (1994). Induction of a dominant negative CREB transgene specifically blocks long-term memory in *Drosophila*. *Cell* 79, 49–58.
- Zhong, Y. (1995). Mediation of PACAP-like neuropeptide transmission by coactivation of Ras/Raf and cAMP signal transduction pathways in *Drosophila*. *Nature* 375, 88–92.
- Zhong, Y., Budnik, V., and Wu, C.-F. (1992). Synaptic plasticity in *Drosophila* memory and hyperexcitability mutants: role of cAMP cascade. *J. Neurosci.* 12, 644–651.
- Zhong, Y., and Wu, C.-F. (1991). Altered synaptic plasticity in *Drosophila* memory mutant with altered cAMP cascade. *Science* 251, 198–201.
- Zhong, Y., and Wu, C.-F. (1993). Differential modulation of potassium currents by cAMP and its long-term and short-term effects: *dunce* and *rutabaga* mutants of *Drosophila*. *J. Neurogenet.* 9, 15–27.
- Zinsmaier, K.E., Eberle, K.K., Buchner, E., Walter, N., and Benzer, S. (1994). Paralysis and early death in cysteine string protein mutants of *Drosophila*. *Science* 263, 977–980.
- Zupan, L.A., Steffens, D.L., Berry, C.A., Landt, M., and Gross, R.W. (1992). Cloning and expression of a human 14-3-3 protein mediating phospholipolysis. Identification of an arachidonyl-enzyme intermediate during catalysis. *J. Biol. Chem.* 267, 8707–8710.